Preprint Title	Solvent-induced assembly of mono- and divalent silica nanoparticles
Authors	Bin Liu, Etienne Duguet and Serge Ravaine
Publication Date	08 Jul 2022
Article Type	Full Research Paper
ORCID® iDs	Etienne Duguet - https://orcid.org/0000-0002-0675-5987; Serge Ravaine - https://orcid.org/0000-0002-6343-8793

Solvent-induced assembly of mono- and divalent silica nanoparticles

Bin Liu[1], Etienne Duguet[2], Serge Ravaine*[1]

[1]Univ. Bordeaux, CNRS, CRPP, UMR 5031, 33600 Pessac, France.

[2]Univ. Bordeaux, CNRS, Bordeaux INP, ICMCB, UMR 5026, 33600 Pessac, France

Email: serge.ravaine@crpp.cnrs.fr

Abstract

Particles with attractive patches are appealing candidates for use as building units in the objective of fabricating novel colloidal architectures by self-assembly. Here, we report the multi-step synthesis of one-patch silica nanoparticles with a well-controlled patch-to-particle size ratio. Their assembly can be triggered by reducing the solvent quality for the polystyrene chains which serve as a patch. Dimers or trimers can be obtained by tuning the patch-to-particle size ratio. When mixed with two-patch nanoparticles, the one-patch nanoparticles control the length of the resulting chains, by behaving as colloidal chain stoppers. The present strategy allows the future elaboration of novel colloidal structures by controlled assembly of nanoparticles.

Keywords

Patchy nanoparticles; assembly; patch-to-particle size ratio; chain stopper

Introduction

Colloidal engineering has become an enormous research effort, with a major focus placed on creating increasingly smart particles scalably, such that desired structures can be assembled in a bottom-up fashion [1-5]. Among all the existing synthetic routes permitting to imbue functionality into a colloidal suspension, those dedicated to the formation of patchy particles have received particular attention [6-10]. Indeed, several generic models including the extended Kern and Kern-inspired patchy models [11-13], the spot-like patchy models [14-15], and the rigid-body patchy models [16-17] have shown the great potentiality of patchy particles to serve as building blocks for the assembly of an exotic variety of colloidal structures. Experimentally, depletion interactions have been utilized to drive particles with a spherical cavity and complementary microspheres to form colloidal clusters [18]. Colloidal chains have been obtained by the assembly of Janus particles with one face selectively functionalized with DNA having self-complementary sticky end [19], particles with two patches functionalized with metal-coordination-based recognition units [20] and by co-assembly of block copolymer micelles and hard nanoparticles [21]. Particles with two patches located at the opposite poles have been assembled into a Kagome lattice by hydrophobic interactions [22], into chains by liquid bridging [23] and into a series of structures under AC electric field [24]. The linear self-assembly of patchy gold nanorods tethered with hydrophobic polymer chains at both ends has been triggered by solvophobic attractions induced by a change in solvent quality [25]. By using post-assembly ligand photo-cross-linking [26] or by adding monofunctional nanospheres into a suspension of bifunctional gold nanorods [27], it was shown that the average degree of polymerization of the resulting chains could be controlled. The reduction of the solvent quality may be also employed to induce the assembly of silica/polystyrene

dumbbells [28] and silica nanoparticles with two PS patches (2-PSN) [29] into multipod-like clusters and colloidal chains, respectively. Here, we report that one-patch silica nanoparticles (1-PSN) with a well-controlled patch-to-particle size ratio (PPSR) assemble into dimers or trimers by following the same strategy. We also show that 1-PSN act as chain stoppers when they are mixed with 2-PSN as the chains tend to be shorter when the amount of 1-PSN increases.

Results and Discussion

Synthesis of one-patch silica particles with well-controlled patch-to-particle size ratio

Figure 1 shows the multi-step approach developed to synthesize 1-PSN with controlled patch size. First, the silica core of the silica/PS monopods used as templates (Figure 2 a) was regrown through successive additions of a small amount of TEOS interspersed with centrifugation/redispersion cycles in order to avoid the occurrence of secondary nucleation of silica. Figures 2 b-f) show the morphology of the silica/PS nanoparticles after 1, 2, 4, 9 and 14 iterative silica growth steps, with measured diameter of the silica cap of 130, 165, 195, 250 and 315 nm, respectively. The second step consisted of the selective dissolution of the physically-entangled PS chains in THF.
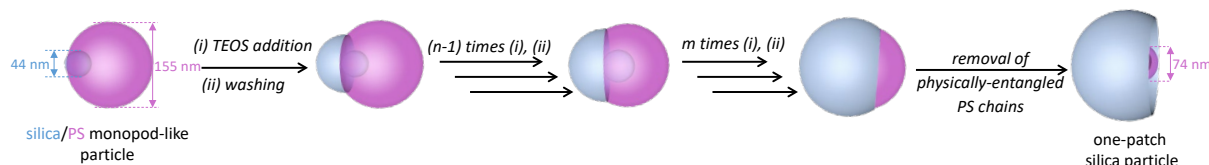

Figure 1: Synthetic route for the preparation of 1-PSN with a controlled patch-to-particle size ratio.
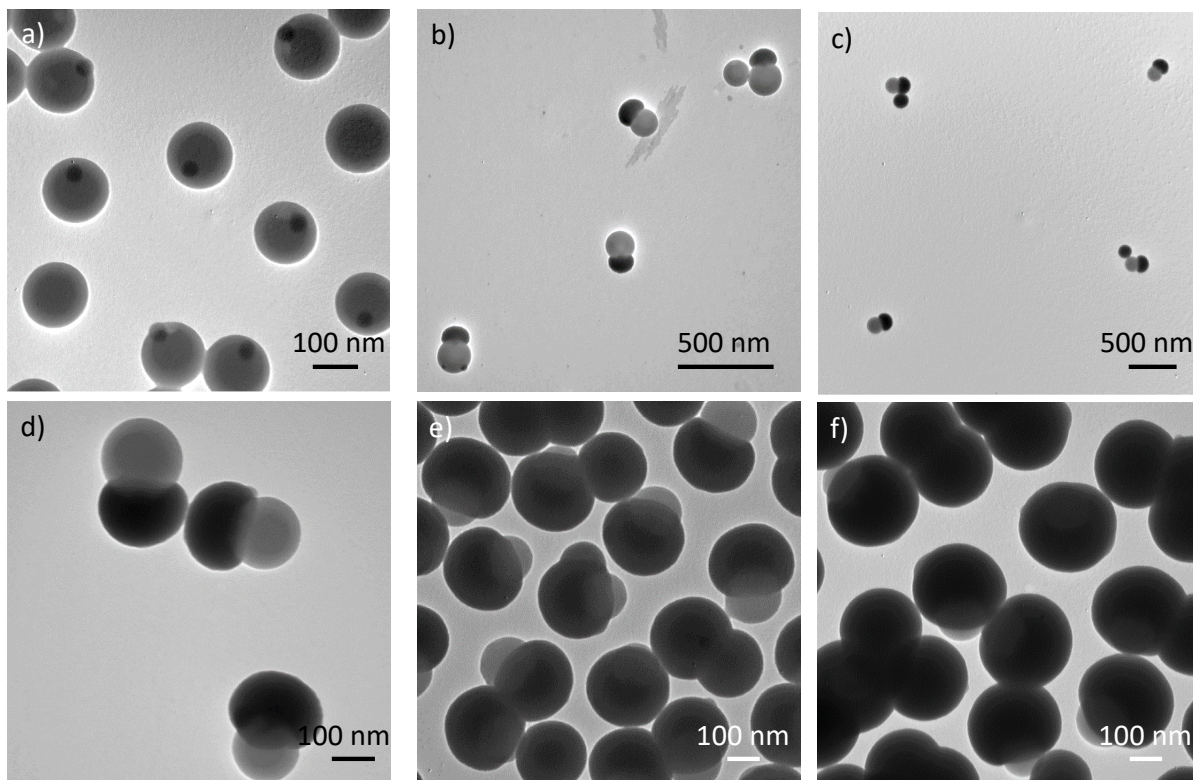
Figure 2: TEM images of the silica/PS monopods after (a) 0, (b) 1, (c) 2, (d) 4, (e) 9, (f) 14 iterative silica growth steps.

As shown in Figure 3, it led to the formation of silica particles with one circular cavity, at the bottom of which the accessible surface of the initial silica seed is decorated by a PS shell of about 15 nm. The latter is made up of covalently grafted PS macromolecules resulting from the copolymerization of styrene with the methacryloxymethyl groups. As demonstrated previously [25], these PS chains can serve as sticky patches when their solubility is reduced through the addition of a bad solvent. Therefore, the PPSR of the as-obtained 1-PSN varies from 0.23 to 0.57 (Figure 3).
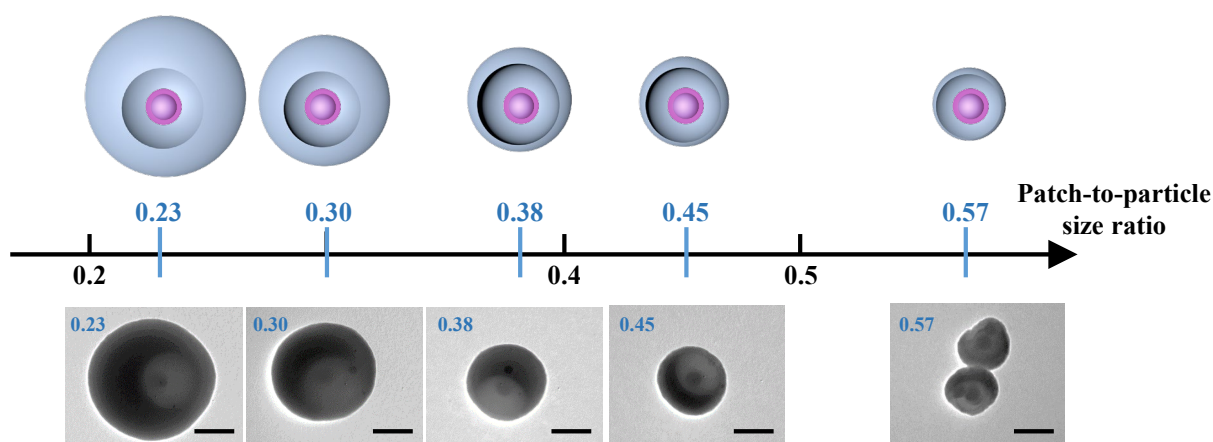
Figure 3: Schemes and representative TEM images of 1-PSN with PPSR varying from 0.23 to 0.57. Scale bars: 100 nm.

Influence of the patch-to-particle size ratio on the self-assembly behaviour of one-patch silica particles

The self-assembly of the 1-PSN dispersed in THF was triggered by the addition of salty water in order to reduce both the electrostatic repulsions between nanoparticles due to negatively charged silanolate groups at their surface and the solvent quality for the PS macromolecules. Minimization of the free surface energy of the system thus corresponded to the formation of physical bonds between the latter [32,33], which thus behave as sticky patches. Figure 4 a) shows that the incubation of 1-PSN with a PPSR of 0.57 in a 7/3 (vol/vol) THF/salty water mixture led to the formation of dimers, trimers and larger aggregates, whose number fraction after 10 days of incubation was 10%, 8% and 74%, respectively. Interestingly, the incubation of 1-PSN with smaller and smaller PPSR progressively led to the formation of assemblies made of fewer and fewer 1-PSN (Figure 4 b-d)). More explicitly, only dimers and trimers were obtained from 1-PSN with a PPSR of 0.45, while only dimers were obtained when PPSR was 0.38.
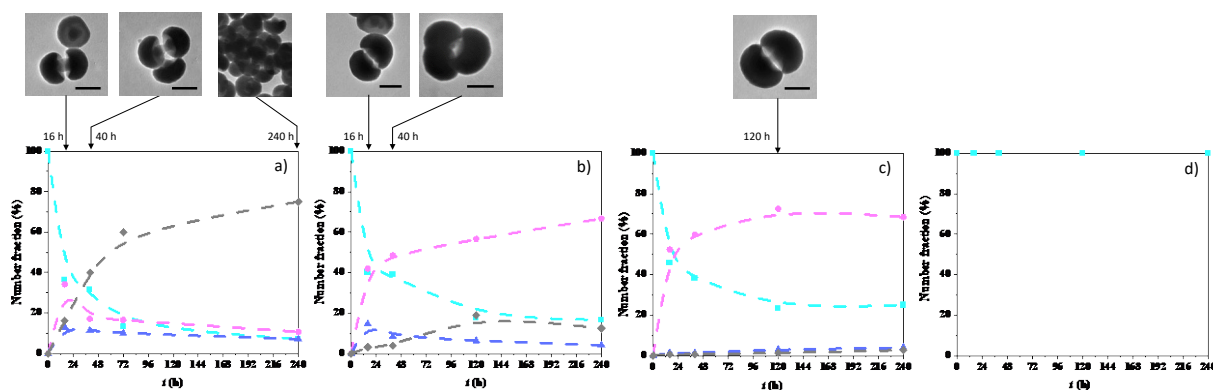
Figure 4: Evolution with incubation time of the fractions of 1-PSN (light blue squares), dimers (magenta circles), trimers (blue triangles) and large clusters (grey diamonds), as determined by statistical analysis of the TEM images for different PPSR values: a) 0.57; b) 0.45; c) 0.38; d) 0.30 or 0.23. Dotted lines are a guide to the eye. Representative TEM images of dimers, trimers and large aggregates formed after 16 h, 40 h, 120 h or 240 h are shown on the top. Scale bars: 100 nm.

Furthermore, no assembly was observed for a PPSR less than or equal to 0.30. These results indicate that the size of the silica cap of the 1-PSN has a strong influence on their capability to self-assemble. Indeed, when the regrown silica cap reaches a certain size, the PS chains which are grafted onto the initial silica seed surface and whose number-average mass was estimated to be ~500 000 gmol-1 [30], can no longer interact because they are too far from each other.

The stickiness of the PS chains in the presence of salty water was further exploited by mixing 1-PSN of two different PPSR. The aim here was not to get heterodimers, i.e. resulting from the assembly of two different 1-PSN, with a high yield since homodimers could also be formed, but to perform a proof-of-principle experiment to demonstrate that such complex structures could be obtained. Figure 5 a) shows that heterodimers were effectively obtained by mixing 1-PSN with a PPSR of 0.45 and 0.38. After 24 hours, the incubation medium consists of 1-PSN (~26%), heterodimers (~30.5%),

homodimers made of two 1-PSN with a PPSR of 0.45 (~17.5%), homodimers made of two 1-PSN with a PPSR of 0.38 (~23%), and also heterotrimers (~1.5%), and homotrimers (~1.5%) (Figure 5 b).
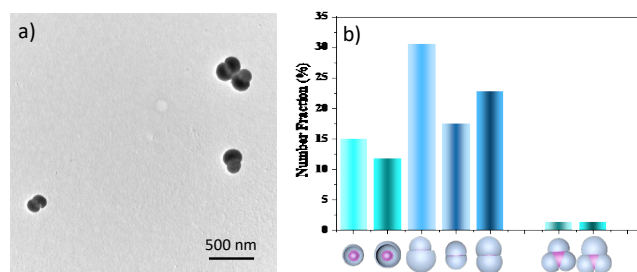

Figure 5: a) TEM image showing some heterodimers obtained after incubation in a 7/3 (vol/vol) THF/salty water mixture during 24 hours of a 1/1 mixture of 1-PSN with a PPSR of 0.45 and 0.38. b) Number fraction of 1-PSN of both sizes, homo- and heterodimers, homo- and heterotrimers present in the incubation medium after 24 hours, as determined by statistical analysis of TEM images.

Co-assembly of 2-PSN and 1-PSN acting as chain-stoppers

It was previously shown that monofunctional nanoparticles can act as chain stoppers, as their addition into suspensions of soft patchy nano-particles [34], gold nanorods [27] or silver nanoplates [35] allowed the control of chain length. We thus studied the capability of the 1-PSN to act as chain stoppers when they are mixed with 2-PSN, whose solvent-induced assembly into colloidal polymers (Figure 6 a)) was recently reported [29]. As shown in Figure 6 c), these divalent nanoparticles, which exhibit a disk-like morphology, formed chains as long as 6 µm after incubation in a 7/3 (vol/vol) THF/salty water mixture. The statistical analysis of the TEM images recorded from samples collected at different incubation times allowed us to plot the time evolution of the number-average degree of polymerization, $\bar{X}_n$, defined as:

$$\bar{X}_n = \frac{\sum n_x x}{\sum n_x},$$

7

where x is the number of 2-PSN in the chain and n_x is the number of chains containing x 2-PSN (Figure 6 b), magenta curve). The linear relationship which can be observed at short incubation time is characteristic of a reaction-controlled step-growth polymerization, in which the reactivity of the patches is independent of the chain length [36]. In order to control the chain length, we added 1 PSN to the suspension of 2-PSN at the particle ratio 0 ≤ 1 PSN/2 PSN ≤ 1.5. Figures 6 c) shows that the chain length depends strongly of the 1 PSN/2 PSN ratio, as the higher it is, the shorter the chains after 120 hours of incubation. The chain stopper strategy allowed us to finely tune the degree of polymerization at any incubation time, as shown in Figure 6 b). For instance, at t = 9 h, the average number of 2 PSN in the chains is 10.7 in the absence of 1 PSN, whereas it is only equal to 3.2, 2.5 and 1.9 when the ratio 1 PSN/2 PSN is 0.5, 1 and 1.5, respectively.

Conclusion

One-patch silica nanoparticles with a controlled patch-to-particle size ratio were synthesized through the conformational enlargement of the silica core of silica/PS monopods. The decrease of the solvent quality for the PS patch made it sticky, which induced the assembly of the patchy silica nanoparticles into mostly dimers when the interactions between the PS chains were not annihilated by steric hindrance between the silica parts. We also show that these one-patch silica nanoparticles can act as colloidal chain stoppers when they are mixed with divalent nanoparticles. We expect these results inspire the fabrication of yet inaccessible colloidal structures by self-assembly. Bridging functionality at the colloidal chain end being now conceivable, their assembly into block-copolymer analogues can for instance be considered.

Figure 6: a) Schematic representation of the solvent-induced assembly of 2-PSN and their co-assembly with 1-PSN. b) Time dependence of $\overline{X}_n$ for 1-PSN/2-PSN = 0 (magenta), 0.5 (light blue), 1 (green) and 1.5 (blue). Curves are a guide to the eye. c) Chain length distribution and representative TEM images of chains for 1-PSN/2-PSN = 0 (magenta), 0.5 (light blue), 1 (green) and 1.5 (blue) at t = 120 h. Scale bars: 200 nm. Experimental conditions are displayed in Table 1.

Experimental details

Materials

We used styrene (Sigma-Aldrich, 99%), methacryloxymethyltriethoxysilane (MMS, ABCR, 98%), sodium persulfate (Sigma-Aldrich, 99%), Symperonic® NP30 (Aldrich), sodium dodecylsulfate (SDS, Sigma-Aldrich, > 90%), tetraethoxysilane (TEOS, Sigma-Aldrich, 99%), L-arginine (98.5 %, Aldrich), ammonium hydroxide (28–30% in water, SDS), sodium hydroxide (98.5 %, microprills) as received. We systematically used ultrapure water with a resistivity of 18.2 MΩ•cm at 25°C obtained from a Milli-Q system (Millipore). We purchased absolute ethanol from VWR Chemicals.

Synthesis of the silica/PS multipods

Monopods consisting of a central silica core attached to one PS nodule have been prepared by seeded-growth emulsion polymerization of styrene, according to a procedure already published [30]. Briefly, silica nanoparticles with an average diameter of 44±2 nm were obtained by TEOS hydrolysis/polycondensation according to a two-stage protocol already published [31]. At the end of the synthesis, the silica surface was functionalized with methacryloxymethyl functions by reacting with MMS at room temperature for 3 hours and then one more hour at 90°C under stirring. The added MMS amount corresponded to a nominal grafting surface density of 0.7 funct./nm^2. Then, the MMS-functionalized silica NPs (1.8×10^{16} part/L) were used as seeds for the seed-growth emulsion polymerization of styrene (100 g/L) stabilized by a mixture (3 g/L) of Symperonic® NP30 and SDS (5 wt.%) and initiated by 1.3 mL $Na_2S_2O_8$ (0.1 g dissolved in 4 mL of water) at 70 °C for 6 h to obtain silica/PS monopods with a PS pod diameter of about 155 nm. The morphological yield was 99%.

Bipods consisting of a central silica core surrounded by two PS nodules were obtained with a yield of 97 % in a similar way from 55±2 nm silica nanoparticles which were functionalized with MMS at 0.5 funct./nm^2.

Controlled growth of the silica core

9.1 mL of absolute ethanol, 0.7 mL of ammonia and 0.2 mL of the dispersion of monopods (1.8×10^{16} part/L) or bipods (1.8×10^{16} part/L) were introduced into a 25-mL flask and the mixture was homogenized using a magnetic bar. 200 µL of TEOS were added all at once after 5 min. The reaction was left under stirring at 20 °C for 15 min. The reaction medium was poured into a 50 mL Falcon tube containing 15 mL of absolute ethanol. After 2 cycles of centrifugation (12,000 g / 5 min) and redispersion in absolute ethanol, the nanoparticles were finally redispersed in 10 mL of a previously prepared hydroalcoholic solution (absolute ethanol/ammonia/water volume ratio: 91%/7%/2%). This protocol was renewed to obtain the next generation.

Dissolution of the PS nodules

For dissolving the PS nodules of the monopods and bipods, three centrifugation/redispersion cycles in 20 mL of THF (12,000 g; 10 min) were performed. The concentration of 1-PSN and 2- PSN dispersions was adjusted to $1.08 \cdot 10^{15}$ part/L and the solution was stored at 4 °C.

Assembly of one-patch silica nanoparticles

Incubation of the nanoparticles was carried out in 15 mL tubes under rolling motion at 60 rpm at room temperature. A calculated volume of salty water (20 mM NaCl aqueous solution) was added drop-by-drop under stirring into the THF dispersion of 1-PSN to reach a volume fraction of 30% and a total volume of 1 mL. It took about 20 seconds for adding 100 µL. Assembled structures were monitored by collecting 50 µL samples at various incubation times and direct deposition on TEM grids.

Co-assembly of one- and two-patch silica nanoparticles

Incubation of the nanoparticles was carried out in 15 mL tubes under rolling motion at 60 rpm at room temperature. The composition of the mixtures is given in Table 1.

Table 1. Experimental conditions used for the co-assembly of 2-PSN and 1-PSN.

1-PSN/2-PSN particle ratio	volume (µL)			
	1-PSN dispersion	2-PSN dispersion	THF	salty water
0	0	700	1400	900
0.5	350	700	1050	900
1	700	700	700	900
1.5	1050	700	350	900

Characterization methods

Transmission electron microscopy (TEM) experiments were performed using a Hitachi H600 microscope operating at an acceleration voltage of 75 kV. We prepared the samples by depositing one drop of the colloidal dispersion on conventional carbon-coated copper grids. We let the liquid evaporate in the open air at room temperature and placed the grids in a box away from dust. Statistics from image analysis were performed over at least 300 multipods or 200 chains. The ζ potential value of 1-PSN aqueous dispersions (pH ~5.7) was measured using the Malvern Zetasizer 3000 HS setup (Malvern Instruments). The dielectric constant of water was set to 80.4 and the Smoluchowsky constant f(ka) was 1.5.

Acknowledgements

References

1   Glotzer, S.; Solomon; M.; Kotov, N. A. *AIChE J.*, **2004**, *50*, 2978−2985.

2   Damasceno, P. F.; Engel, M.; Glotzer, S. C. *Science*, **2012**, *337*, 453−457.

3   Hynninen, A. P.; Thijssen, J. H.; Vermolen, E. C.; Dijkstra, M.; Van Blaaderen, A. *Nat. Mater.*, **2007**, *6*, 202−205.

4   Cademartiri, L.; Bishop, K. J.; Snyder, P. W.; Ozin G. A. *Philos. Trans. R. Soc. A*, **2012**, *370*, 2824−2847.

5   Halverson, J. D.; Tkachenko, A. V. *Phys. Rev. E*, **2013**, *87*, 062310.

6   Ravaine, S.; Duguet, E. *Current Opinion in Colloid &Interface Science*, **2017**, *30*, 45–53.

7   Yi, G. R.; Pine, D. J.; Sacanna, S. *J. Phys. Condens. Matter*, **2013**, *25*, 193101.

8   Du, J.; O'Reilly, R. K. *Chem. Soc. Rev.*, **2011**, *40*, 2402–2416.

9   Pawar, A. B.; Kretzschmar, I. *Macromol. Rapid Commun.*, **2010**, *31*, 150–168.

10   Duguet, E.; Hubert, C.; Chomette, C.; Perro, A.; Ravaine, S. *Comptes Rendus Chim.*, **2016**, *19*, 173–182.

11   Sciortino, F.; Giacometti, A.; Pastore, G. *Phys. Rev. Lett.*, **2009**, *103*, 237801.

12   Giacometti, A.; Lado, F.; Largo, J.; Pastore, G.; Sciortino, F. *J. Chem. Phys.*, **2009**, *131*, 174114.

13   Sciortino, F.; Giacometti, A.; Pastore, G. *Phys.Chem. Chem. Phys*., **2010**, *12*, 11869–11877.

14   Zhang, Z.; Keys, A. S.; Chen, T. Glotzer, S. C. *Langmuir*, **2005**, *21*, 11547–11551.

15   Bianchi E, Largo J, Tartaglia P, Zaccarelli E and Sciortino F 2006 Phys. Rev. Lett. 97 168301.

[16]   Yan LT, Popp N, Ghosh SK and Boker A 2010 ACS Nano 4 913–920.

[17]   Nguyen TD, Phillips CL, Anderson JA and Glotzer SC 2011 Comput. Phys. Commun. 182 2307–2313.

[18]   Sacanna S, Irvine WTM, Chaikin PM and Pine DJ 2010 Nature 464 575–578.

[19]   Oh JS, Lee S, Glotzer SC, Yi GR and Pine DJ 2019 Nat. Commun. 10 3936.

[20]   Wang Y, Hollingsworth AD, Yang SK, Patel S, Pine DJ and Weck M 2013 J Am Chem Soc 135 14064–14067.

[21]   Cui Y, Zhu H, Cai J and Qiu H 2021 Nat Commun 12 5682.

[22]   Chen Q, Bae SC and Granick S 2011 Nature 469 381–384.

[23]   Lyu D, Xu W and Wang Y 2022 Angew. Chem. Int. Ed. 61 e202115076.

[24]   Wang Z, Wang Z, Li J and Wang Y 2021 ACS Nano 15 5439–5448.

[25]   Fava D, Nie Z, Winnik MA and Kumacheva E 2008 Adv. Mater. 20 4318–4322.

[26]   Lukach A, Liu K, Therien-Aubin H and Kumacheva E 2012 J Am Chem Soc. 134 18853–18859.

[27]   Klinkova A, Therien-Aubin H, Choueiri RM, Rubinstein M and Kumacheva E 2013 Proc. Natl. Acad. Sci. 110 18775–18779.

[28]   Li W, Ravaine S and Duguet E 2020 J. Colloid Interface Sci. 560 639–648.

[29]   Li W, Liu B, Hubert C, Perro A, Duguet E and Ravaine S 2020 Nano Res. 13 3371–3376.

[30]   Hubert C, Chomette C, Désert A, Sun M, Tréguer-Delapierre M, Mornet S, Perro A, Duguet E and Ravaine, S. 2015 Faraday Discuss. 181 139–146.

[31]   Désert A, Hubert C, Fu Z, Moulet L, Majimel J, Barboteau P, Thill A, Lansalot M, Bourgeat-Lami E, Duguet E and Ravaine S 2013 Angew. Chem. Int. Ed. 52 11068–11072.

[32]   Liu K, Nie Z, Zhao N, Li W, Rubinstein M and Kumacheva E 2010 Science 329 197–200.

[33]   Choueiri RM, Galati E, Klinkova A, Thérien-Aubin H and Kumacheva E 2016 Faraday Discuss. 191 198–204.

[34]   Gröschel A, Walther A, Löbling TI, Schacher FH, Schmalz H and Müller AHE 2013 Nature 503 247–251.

[35]   Luo B, Smith JW, Wu Z, Kim J, Ou Z and Chen Q 2017 ACS Nano 11 7626–7633.

[36]   Yi C, Yang Y and Nie Z. 2019 J. Am. Chem. Soc. 141 7917–7925.